COMPONENT PART NOTICE

THIS PAPER IS A COMPONENT PART OF THE FOLLOWING COMPILATION REPORT:

TITLE: Proceedings of the Antenna Applications Symposium Held at Urbana, Illinois on 19-21 September 1984. Volume 2.

TO ORDER THE COMPLETE COMPILATION REPORT, USE AD-A153 258.

THE COMPONENT PART IS PROVIDED HERE TO ALLOW USERS ACCESS TO INDIVIDUALLY AUTHORED SECTIONS OF PROCEEDING, ANNALS, SYMPOSIA, ETC. HOWEVER, THE COMPONENT SHOULD BE CONSIDERED WITHIN THE CONTEXT OF THE OVERALL COMPILATION REPORT AND NOT AS A STAND-ALONE TECHNICAL REPORT.

THE FOLLOWING COMPONENT PART NUMBERS COMPRISE THE COMPILATION REPORT:

AD#: AD-P004 620 thru AD#: AD-P004 637

AD#: _____ AD#: _____

AD#: _____ AD#: _____

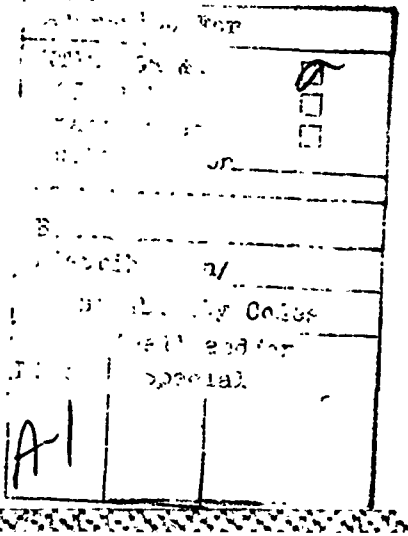

DTIC FORM 463
MAR 85

OPI: DTIC-TID

ANTENNA PHASE CENTRE MOVEMENT IN U.H.F. RADIO POSITIONING SYSTEMS

J.M. Tranquilla and S.R. Best
Department of Electrical Engineering
University of New Brunswick
Fredericton, N.B., Canada
(506) 453-4561

ABSTRACT

Yagi array configurations such as are commonly used in UHF electronic distance measuring (EDM) systems are analysed to show the antenna phase centre movement for any look angle. It is shown that large phase centre movements may occur within the antenna main-beam pattern and the movement of phase centre is directly related to the angular derivative of the polar radiation pattern. A simple technique is proposed for qualitatively estimating the suitability of any antenna for this type of EDM application and a complete model is presented to evaluate the error introduced for any transmitter-receiver antenna orientation. Extensive results are presented for 7- and 12-element Yagis such as are commonly used in the SYLEDIS UHF Radio Positioning System.

1. INTRODUCTION

The radio positioning systems are becoming increasingly popular in such applications as near off-shore positioning (up to a few hundred kilometers) since they offer the advantage of over-the-horizon capability (which limits microwave systems) and more-or-less terrain conductivity-independent propagation path characteristics (which limits lower-frequency systems). A typical example of a modern (UHF system is the SYLEDIS (SYsteme LEgere de DIStance) which operates at 420-450 MHz with stated accuracy of ± 10 m at maximum range (two to three times line-of-sight). Typical antennas used for maximum range are single and stacked 7 and 12-element Yagis.

The major possible error sources associated with the operation of this system can be categorized as propagation (path and cables), electronic and antenna phase centre. Preliminary field trials suggest that the uncertainty of the location of the antenna phase centre (for both the transmitting and receiving antennas) may be the most significant error contribution and may also be most amenable to analysis.

The phase centre of an antenna is, for example in the case of a transmitting antenna, the apparent source of radiation. In the far-field of the antenna (i.e. several wavelengths) the equiphase contours of the radiating electromagnetic wave

describe concentric spherical shells (or portions of sperical shells over defined angular limits) whose geometric centre is at the phase centre of the antenna. Of course, any "distortion" of the spherical wavefront will lead to a movement of the phase centre. This work considers the phase centre movement as a function of frequency and look angle for a variety of commonly used antennas.

Figure 1 depicts a typical radio positioning application. It is required to measure the distance AB between the beacon (at A) and the interrogator (at B). The transmitting antenna at A is permanently pointed in the direction AA'. The receiving antenna at B is not pointed along BA, but rather along BB' which still has sufficient gain at this off-boresight angle to ensure signal reception. The location of the phase centers C and D of the transmitting and receiving antennas respectively are uniquely defined (for a fixed frequency and a particular antenna) by the angles ϕ_2' and ϕ_1' which are the angles between the antennas axes (AA' and BB') and the inter-phase centre line (CD). Of course for each position of the interrogator the phase centers take new positions and hence the angles ϕ_1' and ϕ_2' are different. The distance measured by the equipment in this configuration will be CD which is an erroneous measure of the required distance AB. Thus if A and B are far removed such

that AB is very much larger than the antenna dimensions:

$$\begin{aligned} AB &= AC + BO \\ &\approx CO + AC\ \cos(\theta_2 + \phi_2) + DO + BD\ \cos(\theta_1 + \phi_1) \\ &\approx CD + AC\ \cos(\theta_2 + \phi_2) + BD\ \cos(\theta_1 + \phi_1) \end{aligned} \qquad (1)$$

where the distances AC and BD are functions of the bearing angles ϕ_2' and ϕ_1' respectively and must be determined from an analytical model of the specific antennas. Unfortunately in most (if not all) positioning applications the angles ϕ_1' and ϕ_2' are never determined and hence corrections cannot be made. The problem is aggravated by the fact that phase centre movement may be a sensitive function of these bearing angles.

2. ANTENNA MODEL AND PHASE CENTRE

Figure 2 shows a Yagi array consisting of a driven element, a reflector element and several parasitic director elements. The antenna is described mathematically by a system of equations relating the dipole base currents to the dimensions of the antenna. The base terminals of each of the parasitic dipoles may be considered to be short-circuited since the elements are normally constructed of a single piece of metallic rod. The base of the driven element may be modelled by a voltage or current source with source impedance. The voltage equation at the base of the driven dipoles is then

$$V_T = Z_{DD}I_D + \sum_{\substack{n=1 \\ n\neq D}}^{N} Z_{Dn}I_n, \text{ n an integer} \qquad (2)$$

where N is the number of elements in the array, D is the element number corresponding to the driven element, V_T is the driving voltage at the dipole terminals, Z_{DD} is the self-impedance of the driven element referred to the base, I_D is the driven dipole base current, Z_{Dn} is the mutual impedance between the driven dipole and the n^{th} element in the array referred to the base and I_n is the base current in the n^{th} element. For each of the parasitic elements the voltage equation will be of the same form as (2) with the excitation term on the left-hand side set to zero. Thus we may express the system of voltage equations in matrix form as

$$V = ZI$$

from which

$$I = Z^{-1}V \qquad (3)$$

where Z is the impedance matrix, I is the unknown base current vector and V is the source or excitation vector which is zero except at the driven element where the voltage is arbitrarily set as 1.0 volts. The terms in Z are given by

$$Z_{mn} = -30 \csc \beta h_m \csc \beta h_n \int_{-h_m}^{h_m} [\sin\beta(h_m - |z|)]$$

$$[-j \frac{e^{-j\beta r_1}}{r_2} - j \frac{e^{-j\beta r_2}}{r_2} + 2j \cos \beta h_n \frac{e^{-j\beta r_o}}{r_o}] \, dz \qquad (4)$$

where the dipole dimensions are shown in Figure 3 and the element current is taken to be the filamentary dominant sinusoidal distribution given by

$$I_n(z) = I_n^{max} \sin\beta(h_n - |z|) \qquad (5)$$

where β is the free-space wave number $2\pi/\lambda$. The self impedance terms in (4) are computed by setting d equal to the element radius. Solving (3) for the element base currents thus permits one to compute the far radiation field of the array, thus

$$E = \sum_{n=1}^{N} \int_{-h_n}^{h_n} I_n^{max} \sin(h_n - |z|) \exp(-jkr)$$

$$\exp(-jk \sum_{m=1}^{n-1} d_m \sin\theta \sin\phi) \exp(jkz \cos\theta) \exp(j\omega t) \, dz \qquad (6)$$

This expression for the electric field is a complex quantity which includes all the phase as well as magnitude characteristics of the field. Let $F(\psi, f)$ be the phase quantity associated with

(6) where ψ is an angular variable which describes the "look angle" or "aspect angle" of the antenna and f is the frequency variable. If there exists an origin which reduces $F(\psi, f)$ to a constant then this origin is said to be the phase centre of the antenna. Since this definition of phase centre[1] depends upon polarization and the plane which contains the angular variable ψ, these two quantities must be specified whenever the concept of phase centre is used. In this work the principal θ and ϕ planes (or E and H planes respectively) are of interest.

For most antennas the phase is a function of ψ whatever the origin chosen, but over a limited range of ψ there may exist a point p such that $F(\psi, f)$ is practically constant. If p is chosen as the phase centre for a given aspect angle ψ_p, then the range of ψ for which the fixed point p can be used as the phase centre will depend on the allowable tolerance on F. To find the point p use is made of the evolute of a plane equiphase contour. The evolute is the locus of the centre of curvature of the contour, and the centre of curvature corresponds to the location of an origin which leads to no change in the phase function over an increment $\Delta\psi$. The knowledge of $F(\psi, f)$ as a function of ψ for any origin near the antenna is sufficient to determine the evolute of a far-field equiphase contour.

In the coordinate system of Figure 4, OP = 4 is the distance

from the origin to a point on an equiphase contour S. The ray DP is normal to the tangent line of S at P, therefore DP must pass through the centre of curvature. Using the development of Carrel[1] the displacement of the phase centre can be approximated by

$$\frac{d_i}{\lambda} = -\frac{F(\psi_i + \Delta\psi) \quad F(\psi_i)}{2\pi[\cos(\psi_i + \Delta\psi) - \cos\psi_i]} \tag{7}$$

where ψ_i is a given value of ψ and $\Delta\psi$ is an increment. As $\Delta\psi$ becomes small, equation (7) approximates the derivative of $F(\psi)$ with respect to the variable $2\pi\cos\psi$. Once d is found as a function of ψ, rays such as DP can be drawn by setting $\gamma = \psi$. The evolute of the equiphase contour is then the envelope curve of the rays.

We consider the case shown in Figure 5 to illustrate the features of the phase centre movement. Consider the offset distances d_1, d_2, d_3 corresponding to observation angles ψ_1, ψ_2, ψ_3 respectively and let the rays R_1, R_2, R_3 be the distances from d_1, d_2, d_3 respectively to the intersections with the evolute contour. Let points A and B be the ray intersections of ray pairs R_1, R_2 and R_1, R_3 respectively. If the angular increments between ψ_1, ψ_2 and ψ_1, ψ_3 are small then points A and B will be approximately on the evolute. The distance L can be

computed between the intersection of any consecutive ray pairs and the origin and this distance will be a close approximation to the straight line separation between the origin and the phase centre at any observation angle.

$$L_A = \sqrt{(x_3 + d_2)^2 + (x_3 \tan\psi_2)^2} \tag{8}$$

$$x_3 = \frac{\frac{\tan\psi_1}{\tan\psi_2}(d_2 - d_1)}{1 - \frac{\tan\psi_1}{\tan\psi_2}}, \quad d_1 \text{ and } d_2 \text{ negative to left of 0}$$

where the distances L_A, L_B are assigned to correspond to angles ψ_2 and ψ_1 respectively. Thus for any observation angle ψ_i one may readily locate the phase centre by knowing L_i and the corresponding d_i.

In this work the field is computed at 1 degree angular increments and L is calculated using each successive ray pair.

3. NUMERICAL RESULTS - 12 ELEMENT YAGI

This section describes the radiation characteristics of a 12-element Yagi having dimensions given in Table 1. The computed swept-frequency front and back patterns are shown in Figure 6 from which we select three operating frequencies to illustrate the different types of phase centre behaviour:

frequency point "A" (650 MHz) has moderate front-to-back ratio with shallow sidelobe nulls; frequency point "B" (668.5 MHz) has maximum front-to-back ratio with very deep sidelobe nulls and frequency point "C" (754 MHz) is a resonance[2] which is characterized by scalloping of the main lobe and high side and backlobes. This last point is chosen to illustrate the effects of resonant behaviour and, although the antenna would not normally be operated at its extreme bandedge as in this case, it has been shown[3,4] that similar resonant behaviour may occur thoughout the passband under various conditions. Figure 6 shows the polar H-plane radiation patterns at these three frequencies of interest and Figure 7 presents the distance L as a function

TABLE 1 Yagi Dimensions

No. of elements N = 12

Reflector element length $2h_{12}$ = 23.6 cm

Driven element length $2h_{11}$ = 21.5 cm

Director element length $2h_1 \rightarrow 2h_{10}$ = 18.5 cm

Element radius a = 1.5 mm

Director element spacing $d_1 \rightarrow d_9$ = 9.4 cm

Driven element-director element spacing d_{10} = 6.0 cm

Reflector element-driven element spacing d_{11} = 7.8 cm

Design frequency = 670 MHz

of angles for these same frequencies.

At 650 MHz and 668.5 MHz the phase centre at boresight ($\phi = 90°$) is located approximately 0.6 m back from the front element along the array axis. As the observation angle (ϕ) moves off boresight the phase centre veers off the antenna with the distance, L, from the front element remaining nearly constant with the 3 dB beamwidth of the antenna. As the off-boresight angle increases L may rapidly increase to tens or even hundreds of meters. At the resonance frequency (754 MHz) the phase centre distance L varies rapidly even within the 3 dB beamwidth. Of particular importance are the rapid changes in L which correspond to the polar pattern null positions where a cusp normally occurs in the evolute. Upon closer examination we note that the magnitude of L is related to the angular derivative of the polar plot and hence deep nulls, where the angular drivative of the polar pattern is large, are characterized by large values of L (Figure 7). Furthermore, sharp nulls have nearly discontinuous angular derivatives resulting in a cusp in the evolute. When the angular derivative is small such as when the main lobe is very broad and "flat" then value of L is correspondingly small.

4. NUMERICAL RESULTS - ANTENNAS USED IN SYLEDIS SYSTEM

We consider now 7- and 12-element Yagis which are in use

in the SYLEDIS radio positioning system. Antenna specifications are given in Table 2 and the swept-frequency responses are shown in Figure 8. Polar H-plane radiation plots are also given at the system operating frequency 432 MHz. Since the

TABLE 2 Yagi Dimensions Used in SYLEDIS System

No. of elements N = 7 (or 12)

Reflector element length $2h_7$ = 35.0 cm ($2h_{12}$ = 35.0 cm)

Driven element length $2h_6$ = 30.0 cm ($2h_{11}$ = 30.0 cm)

Director element lengths $2h_1$ = 27.5 cm

$2h_2 \rightarrow 2h_5$ = 30.0 cm ($2h_2 \rightarrow 2h_{10}$ = 30.0 cm

Element radius a = 3.0 mm

Element separation d_1 = 15.5 cm

$d_2 \rightarrow d_5$ = 14.5 cm ($d_2 \rightarrow d_{10}$ = 14.5 cm)

d_6 = 10.2 cm (d_{11} = 10.2 cm)

antennas are normally vertically polarized in use we consider only angular movements in the H-plane of the antenna. The 7-element array has a $\pm$26° 3 dB beamwidth with a first null 52° off boresight. The 12-element array has a $\pm$16.5° 3 dB beamwidth with a first null at 32° off boresight and a much deeper null at 63° off boresight. A plot of L over one angular

quadrant (ϕ = 0 - 90°) for each antenna is given in Figure 9 from which several observations may be made:

i) for a 7-element array L remains nearly constant (approx. 0.4m) over the 3 db beamwidth however for the 12-element array L changes rapidly within a few degrees of boresight;

ii) both arrays showed large rapid phase centre movements of the order of tens of meters over the quadrant;

iii) the phase centre of the longer array veers off the antenna more rapidly than for the shorter array due to the sharper main lobe with nulls nearer to boresight;

iv) although both arrays have well defined nulls off boresight, longer arrays tend to have much sharper nulls (hence larger angular derivatives and discontinuities in the angular derivative) with corresponding large phase centre movements;

v) for both arrays the general features of the "L vs. angle" curve can be readily predicted by observing the polar radiation pattern and visually estimating the relative size of the angular derivative of the plot, particularly noting the occurrence of sharp nulls;

vi) regardless of the array length there is no single range correction term which can be of value in field service short of calculating the exact phase centre location for each bearing angle and frequency.

5. ERROR CORRECTION

Phase centre movements inevitably result in errors in distance determinations since the electronic equipment simply gives a readout proportional to the phase centre separation between transmitting and receiving antennas. In practice, an initial "calibration" reading is often taken over a path of known length and the instrument reading is manually "corrected" to give zero error. This same correction is then applied to all subsequent readings and is intended to account for fixed phase delays in cable lengths and electronic circuitry as well as any propagation effects which may be present. It also includes any phase centre displacement which was present in the calibration procedure. Referring to Figure 10(a) we have an interrogation site at A using a directional antenna whose phase centre can be computed for any look angle and a beacon at B which, for simplicity of discussion, is assumed to have zero phase centre displacement for all angles in the observation plane. The following discussion is easily adapted for any combination of interrogator-beacon antennas if this assumption

is invalid. The calibration reading is a measure of the distance B - PC1 (where PC1 is the phase centre at the calibration boresight look angle) and is "corrected" to give the known distance AB. For reasons which will be discussed shortly it is important that the calibration be done at boresight. When the receiver antenna is turned through the angle ξ to a new look angle the instrument reading will change by the amount $L' \cos \eta$ (assuming A and B are far removed) corresponding to the new phase centre location PC2. A plot of $L' \cos \eta$ as a function of ξ (Figure 11) will thus indicate an "error" function normalized to the calibration setup. If the receiver is then moved to another observation site and the same initial calibration is used care must be taken to ensure that the antenna bearing with respect to the survey line is identical to that used in the calibration setup. In order to use the "error function" curve to correct the instrument readings it thus becomes necessary to record the antenna bearing (pointing direction with respect to the survey line) with each reading. If the beacon antenna also exhibits phase displacement, as would be the case for Yagi arrays which are typically used, then both antenna bearing angles must be recorded and a separate "error function" curve for the beacon antenna must be available. Corrections for phase centre movement must then be applied at both ends of the survey line.

As indicated above the antenna bearing for calibration should be boresight in which case the phase centre lies on the array axis as well as on the survey line (Figure 10(a)). Then, as discussed earlier, the change in instrument reading indicates the distance $L' \cos \eta$. If, however, the boresight angle is not used for calibration (Figure 10(b)) the change in instrument reading corresponding to an angular antenna rotation ξ will be given by $L' \cos \eta'$ with a resulting different of $L'(\cos\eta' - \cos\eta)$. This discrepancy may become significant even when $\eta' - \eta$ is small since L' may become of the order of tens or even hundreds of meters at some angles for the Yagis studied. The following procedure is therefore recommended for obtaining and correcting range data obtained from systems similar to the SYLEDIS system:

1. Perform a boresight calibration measurement over a known path with known beacon antenna bearing. If the beacon antenna exhibits phase centre movement, its "error function" curves for both antennas must be used to correct the readings.
3. For any changes in cabling, antennas or receiver the calibration procedure must be repeated.
4. Since the largest range errors occur in the vicinity of antenna pattern nulls, each antenna used in the system should be accompanied by its polar radiation pattern in

order that beam null readings may be avoided.

6. CONCLUSION

An analytical model has been developed to compute the location of the phase centre of Yagi arrays for any antenna look angle and this model has been used to calculate distance error curves for antennas commonly used in the SYLEDIS system. Yagis are shown to be unsuitable for uncorrected use in UHF radio positioning systems where wide beam coverage is required and it is shown that significant phase centre movement may occur even within the main lobe, particularly for long, high-gain Yagis. Recommendations are made for a calibration and operation procedure which would allow phase centre movement corrections to be made. A simple technique for qualitatively evaluating the suitablity of an antenna for radio positioning applications is presented.

7. REFERENCES

1. Carrel, R.L. (1961) Analysis and Design of the Log-Periodic Dipole Antenna, Technical Report #52, Contract AF33(616)-6079, Antenna Laboratory, University of Illinois, Urbana, Illinois.

2. Tranquilla, J.M. and Balmain, K.G. (1981) Resonance phenomena on Yagi arrays, Canadian Electrical Engineering Journal 6 (no. 2): 9-13.

3. Tranquilla, J.M. and Graham, G.B. (1982) The development of anomalous responses on single tapered and untapered Yagi antennas as a function of antenna length, Canadian Electrical Engineering Journal 7(No. 1): 18-22.

4. Tranquilla, J.M. and Graham, G.B. (1982) Resonance phenomena on non-skewed H-plane multiple-Yagi arrays, Canadian Electrical Engineering Journal (No. 3): 18-23.

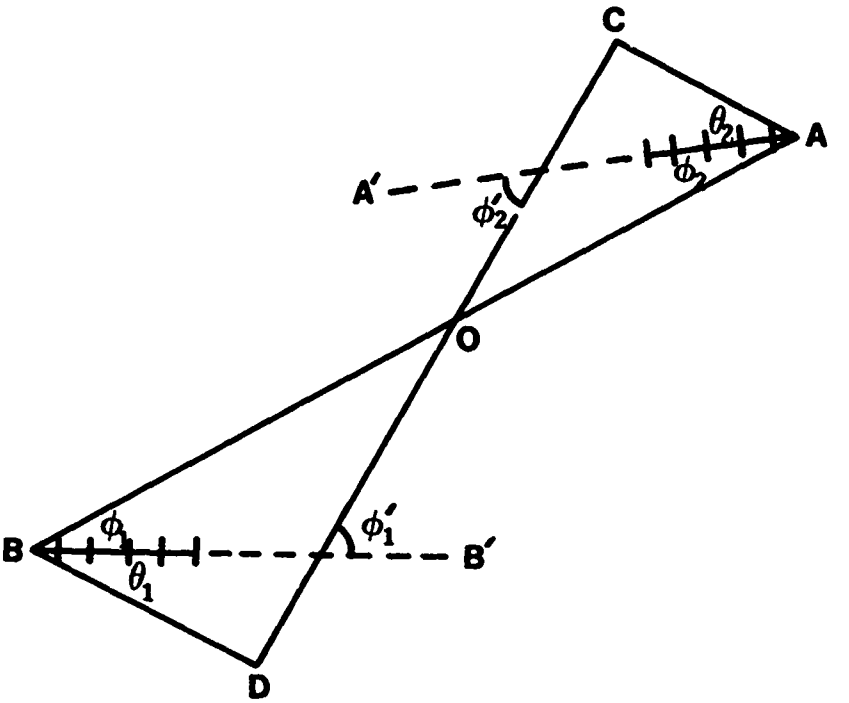

Fig. 1 Typical radio positioning setup with beacon at A, interrogator at B. Phase centres for beacon and receiver antennas are at C and D respectively.

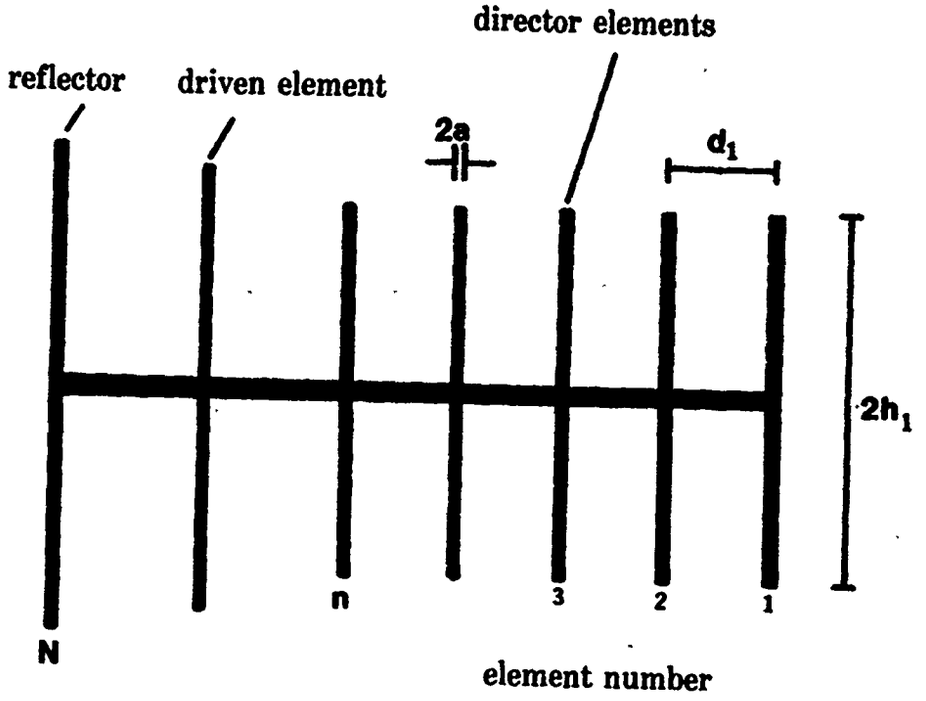

Fig. 2 Yagi array of dipole elements.

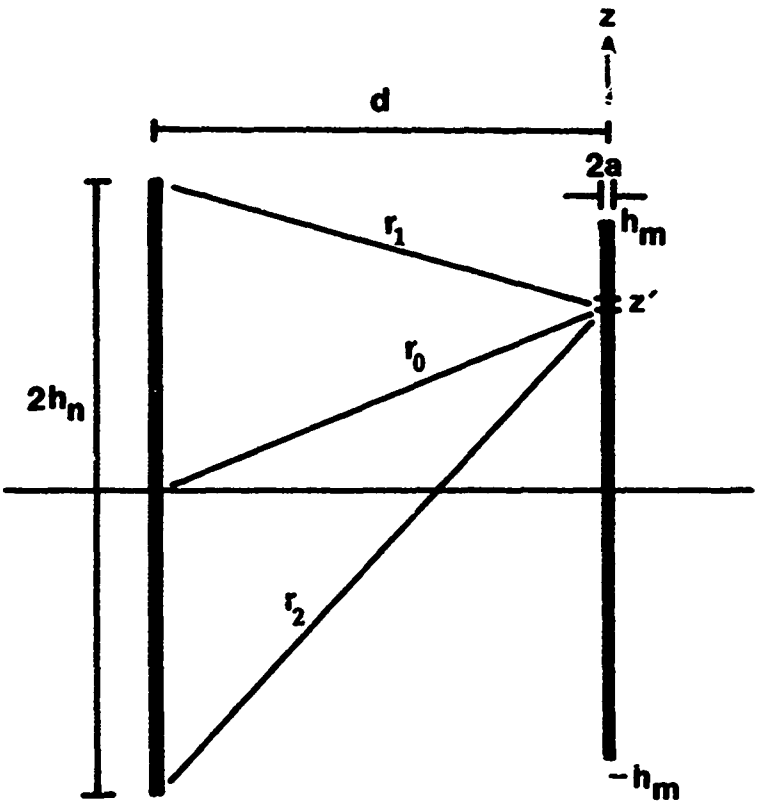

Fig. 3 Geometry for mutual impedance calculation by induced emf method.

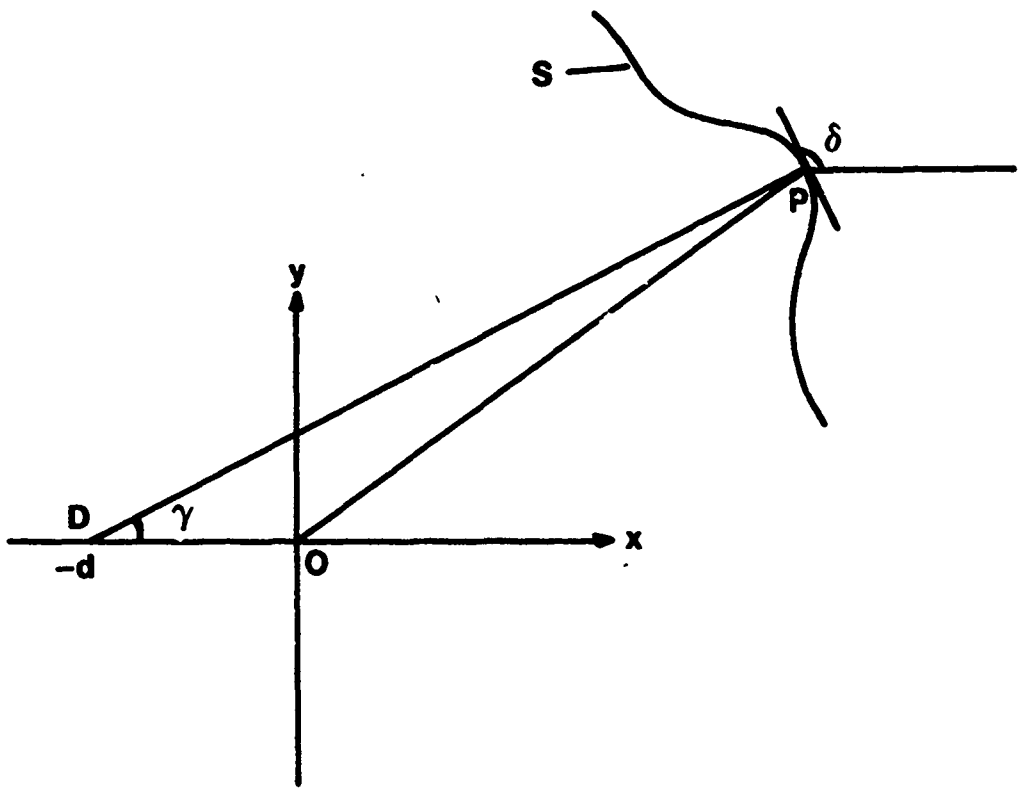

Fig. 4 Coordinate system for phase centre computations (after Carrel [1]).

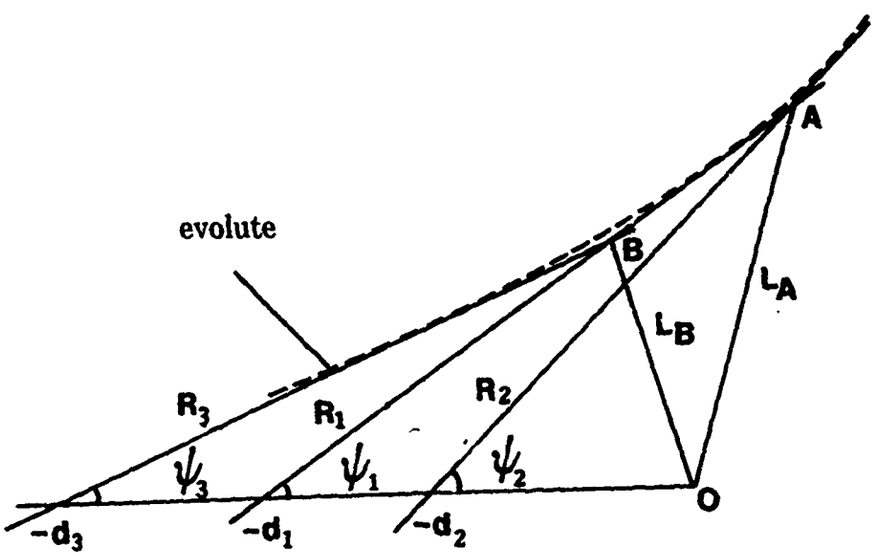

Fig. 5 Geometry for determination of distance from origin tc phase centre.

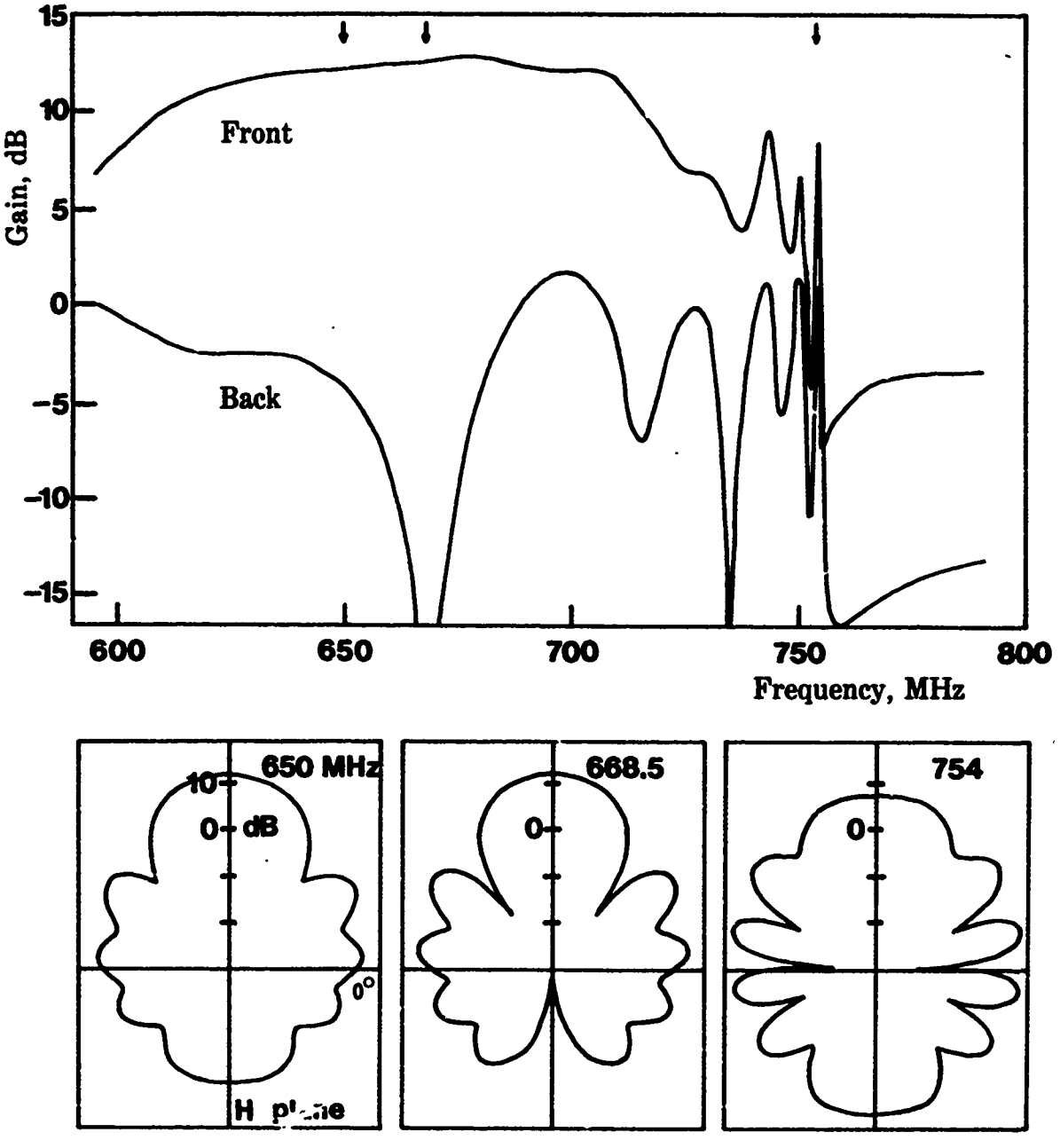

Fig. 6 Calculated swept-frequency radiation pattern for 12-element Yagi and polar patterns at 650 MHz, 668.5 MHz and 754 MHz.

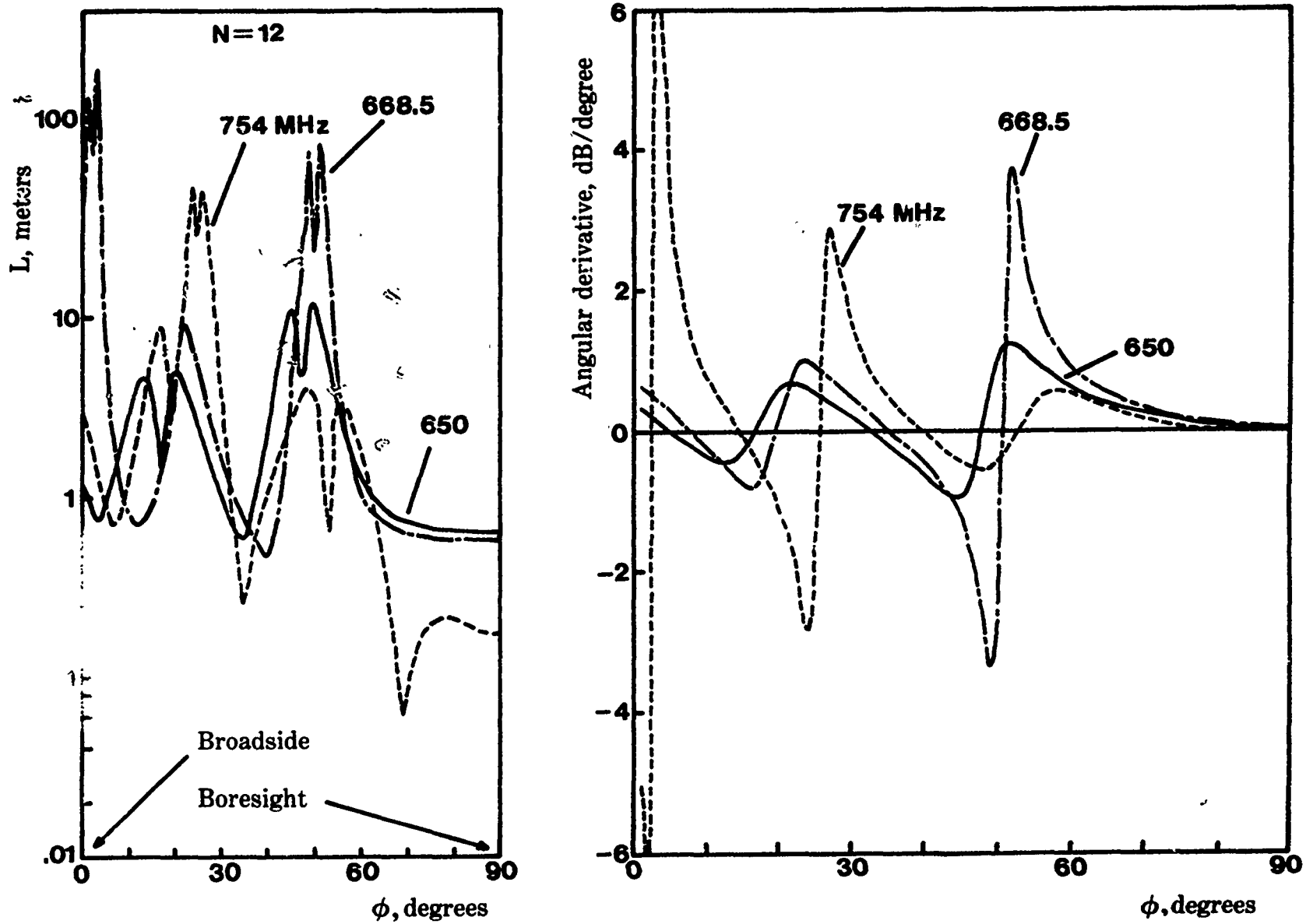

Fig. 7 Calculated phase centre distance L and angular derivative of the polar radiation pattern for 12-element Yagi at 650 MHz, 668.5 MHz and 754 MHz.

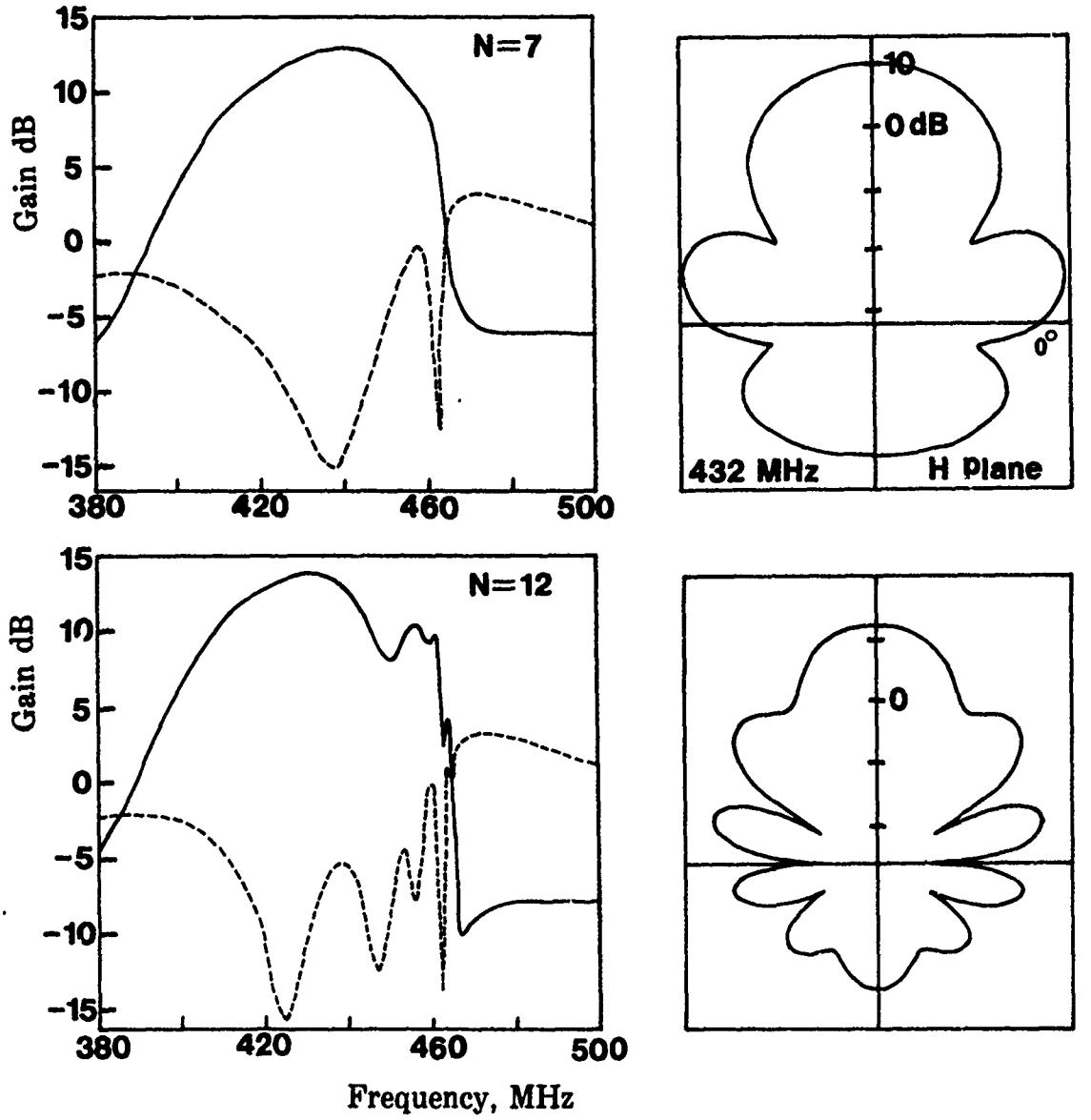

Fig. 8 Calculated swept-frequency radiation pattern for 7 and 12-element Yagi arrays and polar plots for each at 432 MHz.

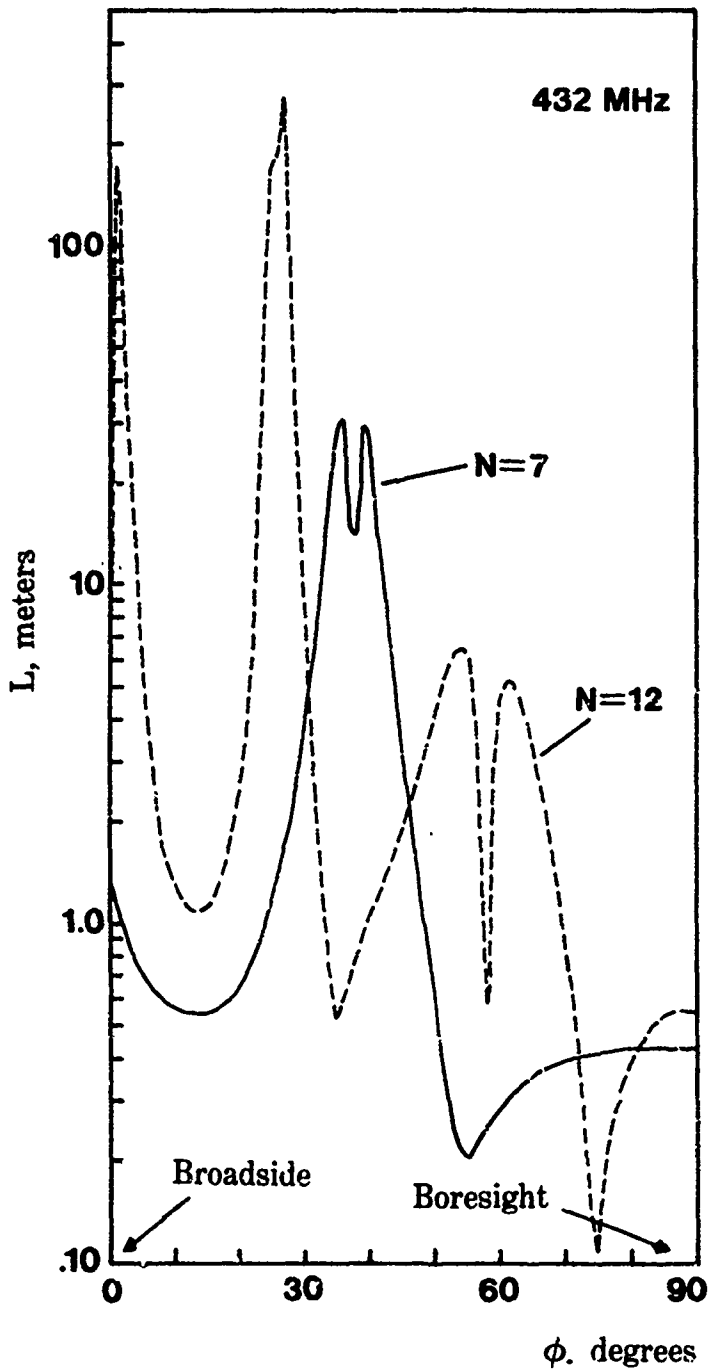

Fig. 9 Computed straight line distance from phase centre to origin for 7 and 12-element Yagi arrays at 432 MHz. Origin is located at the centre of the front director Yagi element.

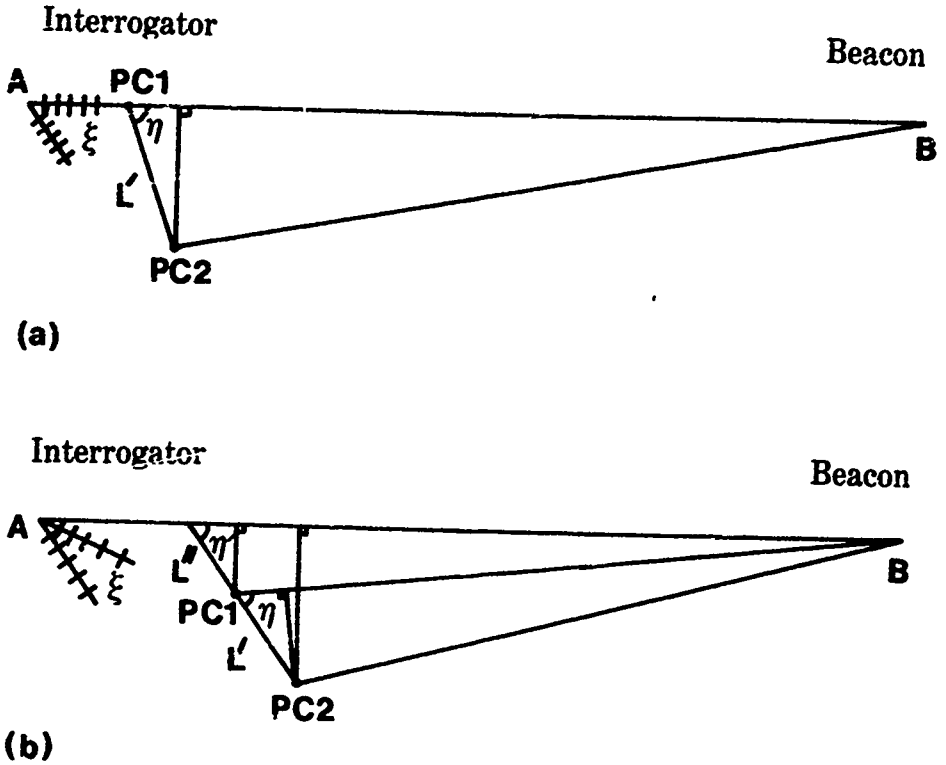

Fig. 10 Error involved in (a) boresight, (b) off-boresight calibration.

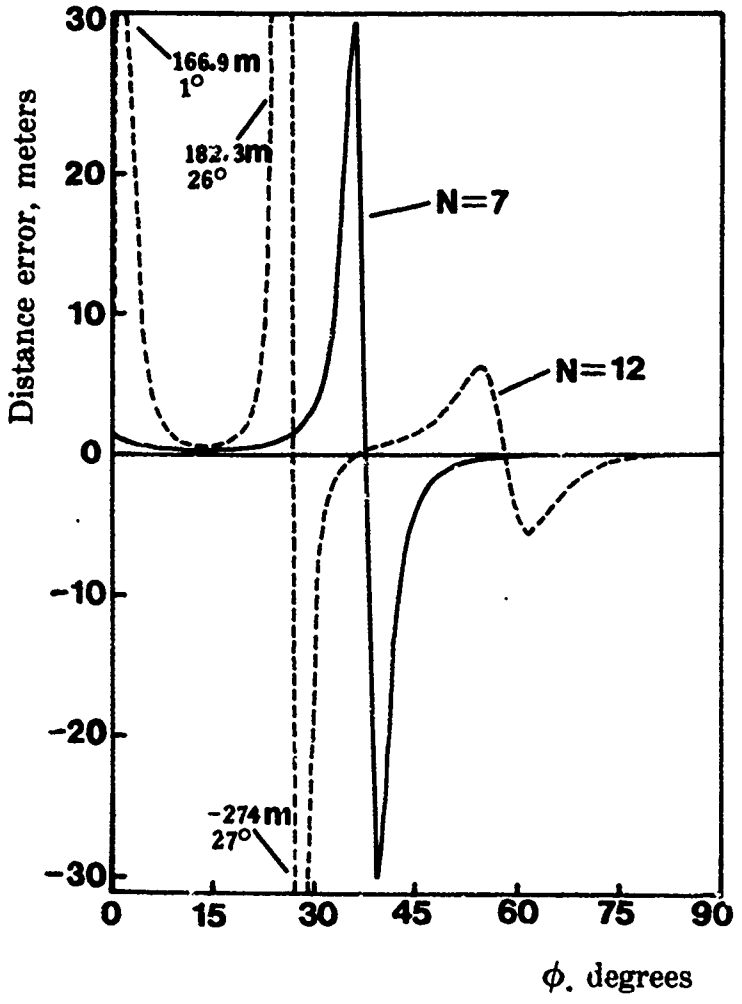

Fig. 11 Computed distance error for 7 and 12-element Yagi arrays at 432 MHz.